JOURNAL OF SOLID STATE CHEMISTRY **132,** 144–150 (1997)
ARTICLE NO. SC977433

Synthesis and Structure of $Cs[(VO)_2(OH)(O_3PCH_2CH_2PO_3)]$: A Two-Dimensional Solid with Pillared Layers

Grant H. Bonavia,* Robert C. Haushalter,† Sichu Lu,‡ Charles J. O'Conner,‡ and Jon Zubieta*,[1]

** Department of Chemistry, Syracuse University, Syracuse, New York 13244; † NEC Research Institute, 4 Independence Way, Princeton, New Jersey 08540; and ‡ Department of Chemistry, University of New Orleans, New Orleans, Louisiana 70148*

Received January 24, 1997; accepted April 15, 1997

The title compound $Cs[(VO)_2(OH)(O_3PCH_2CH_2PO_3)]$ 1 was synthesized hydrothermally from a mixture of $CsVO_3$, $H_2O_3PCH_2CH_2PO_3H_2$, and H_2O in the mole ratio 1 : 1.22 : 535 and heated to 200°C for 48 hr. Phosphonate 1 is formed in 45% yield and crystallizes in the monoclinic space group $P2_1/c$ with $a = 11.798(2)$ Å, $b = 11.056(2)$ Å, $c = 8.682(2)$ Å, $\beta = 104.92(3)°$, $V = 1094.3(4)$ Å^3, $Z = 4$, and $R = 0.054$. The framework consists of complimentary inorganic V/P/O layers joined by ethylenediphosphonate ligands, creating an inorganic bilayer. The bilayers are seperated by an interlamellar region of Cs^+ cations. There are two unique VO_5 square pyramids from which the inorganic V/P/O layers are constructed.

INTRODUCTION

The continuing research in the chemistry of metal–organophosphonates (1–3) can be attributed to the diversity of interesting structures associated with this class of material, as well as to their practical applications, for example, as catalysts (4) and ion exchangers (5, 6). A comparison of a variety of these layered structure types is contained in Table 1. A prototypical oxovanadium organodiphosphonate material $[(VO)_2(H_2O)_4(O_3PCH_2PO_3)]$ **2** (7) is a layered phase containing void spaces as well as open coordination sites that could allow for the association of a substrate to the metal site in the V/P/O layers. Such features are crucial in the design of effective catalysts or sorptive materials. It is noteworthy, in this regard, that the prototypical layered oxovanadium organophosphonate $[VO(O_3PPh)(H_2O)]$ **3** (8, 9) selectively intercalates alcohols by coordination of the substrate to the vanadium atom of the inorganic layers.

In our studies of the metal–organophosphonate systems, we have noted that minor variations in the reaction conditions used to synthesize these solids may have profound influences on the product composition and structure. Investigations of the vanadium–phenylphosphonate system have produced $(C_2H_5NH_3)_2[(VO)_3(H_2O)(PhPO_3)_4]$ **4** (10) which is a layered solid constructed from organophosphonate bridged trinuclear $\{(VO)_3(H_2O)\}^{6+}$ units. Another variation on the vanadium–phenylphosphonate system gives the layered solid $[(C_2H_5)_2NH_2][(CH_3)_2NH_2][(VO)_4(OH)_2(C_6H_5PO_3)_4]$ **5** (11) which is composed of discrete binuclear $\{(VO)_2(OH)\}^{2+}$ units bridged through phosphonate tetrahedra. This structural variability has prompted us to extend the vanadium–organophosphonate system by investigating the influences of templates, tether structures, and reaction conditions. Encouraged by our success with the $CsVO_3$/methylenediphosphonate system, represented by the layered $Cs[(VO)_2V(O_3PCH_2PO_3)_2(H_2O)_2]$ **6** solid (12), we have examined the $CsVO_3$/ethylenediphosphonate system, which reveals the significant structural consequences of introducing an additional methylene group into the tether. In this paper we report the synthesis and characterization of $Cs[(VO)_2(OH)(O_3PCH_2CH_2PO_3)]$ **1**. The structure of **1** consists of inorganic V/P/O layers tethered by bifunctional $(O_3PCH_2CH_2PO_3)^{4-}$ units. This motif creates a an organic/inorganic composite constructed from two inorganic V/P/O layers tethered by organic $\{–CH_2–CH_2–\}$ units. The Cs^+ cations occupy positions in the interlamellar region and are coordinated to oxygen atoms within the inorganic layers.

EXPERIMENTAL

Synthesis. The title compound was hydrothermally synthesized from a mixture of 100 mesh $CsVO_3$ (0.115 g, 0.52 mmol), $H_2PO_3(CH_2)_2PO_3H_2$ (0.060 g, 0.32 mmol), and H_2O (5 ml, 277 mmol). The mixture, in the mole ratio of $CsVO_3 : H_2PO_3(CH_2)_2PO_3H_2 : H_2O$ of 1.00 : 0.62 : 535, was heated in a 23-ml polytetrafluoroethylene lined vessel at 200°C for 48 hr. This afforded light blue hexagonal shaped plates of the title compound. The crude product was washed with distilled water several times, and the yield was found to be ca. 45% based on the total amount of vanadium. A small

[1] To whom correspondence should be addressed.

0022-4596/97 $25.00

TABLE 1
Structural Features of Layered Vanadium-Organodiphosphonate Phases

Compound	Vanadium coordination and linkage	Cell parameters	Space group	V=O_t	V–$O_{phosphonate}$	V–O_{other} (type)	References
$Ca[(VO)_2(OH)(O_3PCH_2CH_2PO_3)]$ **(1)**	Binuclear units of corner-sharing V(IV) square pyramids	11.798(2) 11.056(2) 8.682(2) $\beta = 109.52(3)$	P21/c	1.586(9)	1.971(11) (×4)	2.017(10) (bridging OH)	
$[(VO)_2(O_3PCH_2PO_3)(H_2O)_4]$ **(2)**	Isolated V(IV) octahedra	12.805(4) 10.592 (3) 15.037(5)	Pbca	1.606(3) (VI) 1.619(2) (V2)	1.993(3) (×2) 2.021(3) (×4)	2.103(4) (aquo ×3) 2.215(2) (aquo)	7
$[VO(O_3PPh)(H_2O)]$ **(3)**	Chains of corner-sharing V(IV) octahedra	28.50(3) 7.18(2) 9.42(2) $\beta = 97.1(2)$	C2/c	1.606(3)	1.96(1) (×3)	2.11(1) (aquo) 2.14(1) (V ⋯ O=V)	8,9
$(H_3NEt)_2[(VO)_3(H_2O)(O_3PPh)_4]$ **(4)**	Trinuclear units of corner-sharing V(IV) octahedra	14.708(3) 12.406(2) 10.275(2) $\beta = 93.66(1)$	$P2_1/n$	1.62(1) (VI) 1.53(1) (V3)	1.981(8) (×4) 2.006(8) (×4)	2.676(7) (V ⋯ O=V) 2.162(9) (V ⋯ O=V)	10
$(H_2NEt_2)(H_2NMe_2)[(VO)_4(OH)_2(O_3PPh)_4)]$ **(5)**	Binuclear units of corner-sharing V(IV) square pyramids	21.022(4) 19.034(3) 10.771(2) $\beta = 99.63(2)$	$P2_1/n$	1.53(1)	1.958(9) (×3)	1.96(1) (bridging OH)	11
$Cs[(VO)_2V(O_3PCH_2PO_3)_2(H_2O)_2]$ **(6)**	Trinuclear units of corner-sharing V(IV) and V(III) octahedra	9.724(2) 8.136(2) 10.268(2) $\beta = 103.75(3)$	C2/m		1.97(1) (×4) 1.99(1) (×6)	1.783(9) (bridging oxo) 2.14(1) (aquo)	12
$(H_3O)_2[(VO)V_2(OH)_2(O_3PCH_2CH_2PO_3)_2 \cdot H_2O$ **(7)**	Chains of corner-sharing V(III) octahedra and isolated V(IV) square pyramids	7.150(1) 7.809(2) 9.996(2) 76.55(2) 70.17(2) 88.91(2)	$P\bar{1}$	1.53(2)	1.981(7) (×4) 1.95(1) (×4)	1.924(9) (bridging OH ×2)	20
$[(VO)\{O_3PCH_2NH(C_2H_4)_2NHCH_2PO_3\}(H_2O)]$ **(8)**	Isolated V(IV) octahedra	7.999(2) 8.009(2) 9.201(2) $\beta = 100.24(3)$	$P2_1/c$	1.578(4)	2.008(3) (×4)		21
$(H_2en)[(VO)_4(OH)_2(H_2O)_2(O_3PCH_2CH_2CH_2PO_3)_2] \cdot 4H_2O$ **(9)**	Binuclear units of corner-sharing V(IV) square pyramids and octahedra	14.870(3) 10.245(2) 18.868(4) $\beta = 99.50(3)$	C2/c	1.583(7) 1.615(8)	1.971(8) (×3) 1.993(8) (×3)	1.930(7) (bridging OH) 1.9995(7) (bridging OH) 2.388(9) (aquo)	22

amount of side product was formed in the initial synthesis. The suppression of the side product was accomplished by the addition of 2.5 ml of a 0.1 *M* solution of $CsOH \cdot H_2O$ in H_2O. IR (KBr pellet, $\nu(cm^{-1})$): 3461 (s), 2914 (w), 1201 (s), 1159 (s), 1053 (vs), 998 (vs), 777 (m), 727 (m).

Crystallography. The structural study of phosphonate **1** was performed on a Rigaku AFC5S diffractometer with graphite monochromated Mo$K\alpha$ radiation [λ (Mo$K\alpha$) = 0.71073 Å]. The data were collected at a temperature of $20 \pm 1^\circ$C using the ω-2θ scan technique to 55° in 2θ at a scan speed of 8°/min (in omega). Crystallographic data for the compound are listed in Table 2. The intensities of three standard reflections measured after every 150 reflections remained constant throughout the data collections. An empirical absorbtion correction using the program DIFABS

TABLE 2
Crystallographic Data for $Cs[(VO)_2(OH)(O_3PCH_2CH_2PO_3)]$ (1)

Formula	$C_2H_5CsO_9P_2V_2$
Space group	$P2_1/c$
a, Å	11.798(2)
b, Å	11.056(2)
c, Å	8.682(2)
β, °	104.92(3)
V, Å	1094.3(4)
D_{calc}, g cm^{-3}	2.845
Z	4
μ, cm^{-1}	53.07
T, K	293
λ, Å	0.71073 (Mo$K\alpha$)
R^a	0.054
$R_w{}^b$	0.053
Goodness-of-fit	1.69
Largest difference peak, eÅ^{-3}	1.56
Largest difference hole, eÅ^{-3}	− 1.14

[a] $R = \sum||F_o| - |F_c|| / \sum|F_o|$.
[b] $R_w = [\sum[w(F_o - F_c)^2] / \sum w(F_o)^2]^{1/2}$; $w^{-1} = \sigma^2(F) + 0.0001\ F^2$.

was applied to all data (13), and the data were corrected for Lorentz and polarization effects. The structure was solved by direct methods (14). Refinement was by full-matrix least squares on F^2. Vanadium and oxygen atoms were refined anisotropically. Hydrogen atoms were fixed in positions of ideal geometry. Neutral atom scattering factors were taken from Cromer and Waber (15) and the anomalous dispersion correction was taken from those of Creagh and McAuley (16). All calculations were performed using the SHELXTL (17) crystallographic software package.

Magnetism. The magnetic susceptibility data were recorded on a 16.02-mg polycrystalline sample of $Cs[(VO)_2(OH)(O_3PCH_2CH_2PO_3)]$ over the 2–300 K temperature region using a Quantum Design MPMS-5S SQUID susceptometer. Measurement and calibration techniques have been reported elsewhere (18). The temperature dependent magnetic data were measured at a magnetic field of 1000 G.

RESULTS AND DISCUSSION

The title compound was synthesized hydrothermally using $CsVO_3$, $H_2PO_3(CH_2)_2PO_3H_2$, and H_2O in the molar ratio 1.00 : 0.62 : 535. Hydrothermal synthesis provides a low-temperature route to metastable phases as well as an effective method of introducing a wide range of starting materials, since all precursors are soluble at the 150–250°C temperature range under autogenous pressure. Reflecting Ostwald's rule, kinetic barriers dictate the metastable phase as energetically more stable with respect to thermodynamic phases (19). In order to obtain a monophasic product, the pH of the initial reaction mixture was raised to 5 with a 0.1 M solution of $CsOH \cdot H_2O$ in H_2O. The infrared spectrum of **1** is characterized by strong bands at 1159 and 1053 cm^{-1}, assigned to stretching modes of the $-PO_3^{2-}$ unit, and a sharp band at 998 cm^{-1}, assigned to ν(V=O).

Atomic positional parameters and selected bond lengths and angles are presented in Tables 3 and 4, respectively. The structure of **1** consists of a two-dimensional anionic framework built up from complimentary V/P/O layers which are joined through the organic component of the diphosphonate ligand. This pillaring is evident in a number of previously synthesized oxovanadium diphosphonate solids. Some examples are the layered materials $(H_3O)_2[(VO)V_2(OH)_2(O_3PCH_2CH_2PO_3)_3] \cdot H_2O$ **7** (20) and $[(VO)(H_2O)\{O_3PCH_2NH(C_2H_4)_2NHCH_2PO_3\}]$ **8** (21). In the title compound, these bilayers are separated by an interlamellar region populated by Cs^+ cations. The inorganic V/P/O layers are composed of VO_5 square pyramids and RPO_3^{2-} tetrahedra as seen in Fig. 1. There are two distinct VO_5 square pyramids, which are linked through a hydroxyl bridge (O6) to form isolated $\{(VO)_2(OH)\}$ binuclear units in the V/P/O layer. This binuclear unit is also evident in the oxovanadium diphosphonate $[H_2N(CH_2CH_2)_2NH_2][(VO)_4(OH)_2(H_2O)_2\{O_3P(CH_2)_3PO_3\}_2] \cdot 4H_2O$ **9** (22) which exhibits a layer motif very similar to that of **1**. The coordination about the V1 square pyramidal site consists of an apical vanadyl oxygen (O5), three diphosphonate oxygens (O1, O3, O9), and the bridging hydroxyl oxygen. The

TABLE 3
Atomic Positional Parameters ($\times 10^4$) and Isotropic Temperature Factors (Å $\times 10^3$) for $Cs[(VO)_2(OH)(O_3PCH_2CH_2PO_3)]$ 1

	x	y	z	U(eq)[a]
Cs(1)	9426 (1)	− 1442 (1)	− 2257 (1)	30 (1)
V(1)	12266 (2)	720 (2)	− 917 (2)	12 (1)
V(2)	17755 (2)	1110 (2)	4385 (2)	13 (1)
P(1)	13039 (3)	− 1224 (3)	2120 (3)	14 (1)
P(2)	16828 (3)	− 1710 (3)	3840 (4)	14 (1)
O(1)	17518 (8)	− 2799 (8)	4566 (9)	22 (3)
O(2)	12451 (7)	− 1457 (8)	3446 (8)	19 (3)
O(3)	16823 (8)	− 1632 (7)	2073 (9)	23 (3)
O(4)	19135 (8)	1278 (9)	4754 (10)	32 (4)
O(5)	10902 (8)	843 (8)	− 1712 (10)	28 (3)
O(6)	12667 (8)	− 742 (7)	− 1990 (9)	19 (3)
O(7)	13034 (7)	− 2356 (7)	1108 (9)	18 (3)
O(8)	17292 (8)	− 562 (7)	4757 (9)	20 (3)
O(9)	12441 (8)	− 175 (7)	1066 (9)	20 (3)
C(1)	14540 (11)	− 825 (11)	2910 (14)	22 (3)
C(2)	15305 (11)	− 1867 (11)	3815 (14)	20 (3)

[a] Equivalent isotropic U defined as one third of the trace of the orthogonalized U_{ij} tensor.

TABLE 4
Selected Bond Lengths (Å) and Angles (°) for $Cs[(VO)_2(OH)(O_3PCH_2CH_2PO_3)]$ 1

V(1)–O(5)	1.585 (9)	V(1)–O(6)	1.983 (8)
V(1)–O(9)	1.950 (8)	V(1)–O(1B)	1.992 (8)
V(1)–O(3A)	1.933 (10)	V(2)–O(4)	1.588 (9)
V(2)–O(8)	1.977 (8)	V(2)–O(2A)	1.996 (8)
V(2)–O(6A)	2.050 (8)	V(2)–O(7A)	1.929 (8)
P(1)–O(2)	1.512 (9)	P(1)–O(7)	1.529 (9)
P(1)–O(9)	1.531 (8)	P(1)–C(1)	1.782 (12)
P(2)–O(1)	1.498 (9)	P(2)–O(3)	1.535 (9)
P(2)–O(8)	1.524 (8)	P(2)–C(2)	1.799 (13)
C(1)–C(2)	1.548 (16)		
O(5)–V(1)–O(6)	101.7 (4)	O(5)–V(1)–O(9)	107.0 (4)
O(6)–V(1)–O(9)	91.0 (3)	O(5)–V(1)–O(1B)	98.5 (4)
O(6)–V(1)–O(1B)	159.6 (4)	O(9)–V(1)–O(1B)	85.9 (3)
O(5)–V(1)–O(3A)	111.5 (4)	O(6)–V(1)–O(3A)	87.1 (4)
O(9)–V(1)–O(3A)	141.0 (4)	O(1B)–V(1)–O(3A)	82.7(4)
O(4)–V(2)–O(8)	112.9 (4)	O(4)–V(2)–O(2A)	98.9 (4)
O(8)–V(2)–O(2A)	85.4 (4)	O(4)–V(2)–O(6A)	101.3 (4)
O(8)–V(2)–O(6A)	88.6 (3)	O(2A)–V(2)–O(6A)	159.7 (4)
O(4)–V(2)–O(7A)	110.6 (4)	O(8)–V(2)–O(7A)	136.1 (4)
O(2A)–V(2)–O(7A)	82.6 (4)	O(6A)–V(2)–O(7A)	88.4 (3)
O(2)–P(1)–O(7)	111.3 (5)	O(2)–P(1)–O(9)	110.7 (5)
O(7)–P(1)–O(9)	110.1 (4)	O(2)–P(1)–C(1)	110.7 (5)
O(7)–P(1)–C(1)	106.3 (5)	O(9)–P(1)–C(1)	107.6 (5)
O(1)–P(2)–O(3)	109.1 (5)	O(1)–P(2)–O(8)	111.5 (4)
O(3)–P(2)–O(8)	112.6 (5)	O(1)–P(2)–C(2)	111.1 (6)
O(3)–P(2)–C(2)	104.3 (5)	O(8)–P(2)–C(2)	108.0 (6)
P(2)–O(1)–V(1D)	151.8 (7)	P(1)–O(2)–V(2C)	151.2 (5)
P(2)–O(3)–V(1B)	133.5 (5)	V(1)–O(6)–V(2B)	127.8 (4)
P(1)–O(7)–V(2D)	141.1 (6)	V(2)–O(8)–P(2)	140.4 (5)
V(1)–O(9)–P(1)	147.0 (6)	P(1)–C(1)–C(2)	113.8 (9)
P(2)–C(2)–C(1)	112.6 (9)		

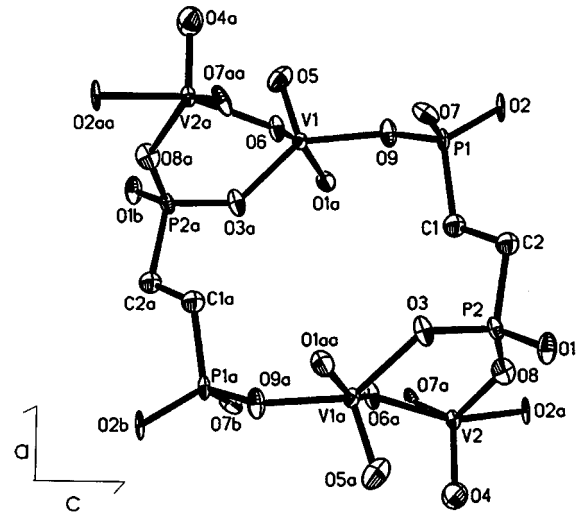

FIG. 1. A view of the repeating structural motif of $Cs[(VO)_2(OH)(O_3PCH_2CH_2PO_3)]$ **1**, showing the atom-labeling scheme and the 50% probability ellipsoids.

coordination of the V2 site is analogous to V1. Valence bond calculations (23) confirm that both vanadium centers are present in the + 4 oxidation state.

Multiple ring systems exist within the V/P/O layers. There are 6-, 10-, and 12-membered rings in the layer as seen in Fig. 2. The 6-membered ring is composed of a hydroxyl bridged binuclear unit which is joined through the oxygens of a RPO_3^{2-} unit. The 10-member ring is created by the binuclear unit as well as two RPO_3^{2-} units and a third VO_5 square pyramid from a neighboring binuclear unit. The 12-member ring is composed of three RPO_3^{2-} units and three VO_5 square pyramids of different binuclear units joined in an alternating fashion.

The V/P/O layers, parallel to the *bc* plane, are joined via the ethylene diphosphonate groups as shown in Fig. 3. The diphosphonate ligand joins six vanadium centers as illustrated in Fig. 4. The $-PO_3^{2-}$ unit of P1 connects three vanadium centers of three different binuclear units (V1, V2a, and V2b), while the $-PO_3^{2-}$ unit of P2 links two vandium centers of a single binuclear unit (V1b and V2) and the third of a neighboring binuclear unit (V1a). This motif of complimentary inorganic layers joined by an organic tether creates an inorganic bilayer separated by organic ethylene fragments. An interesting consequence of this pattern is that the vanadyl oxygens are all oriented toward the interlamellar region. This would seem to create hydrophobic and hydrophilic areas within the solid. The vanadyl oxygens coordinate to Cs^+ cations between bilayers. This

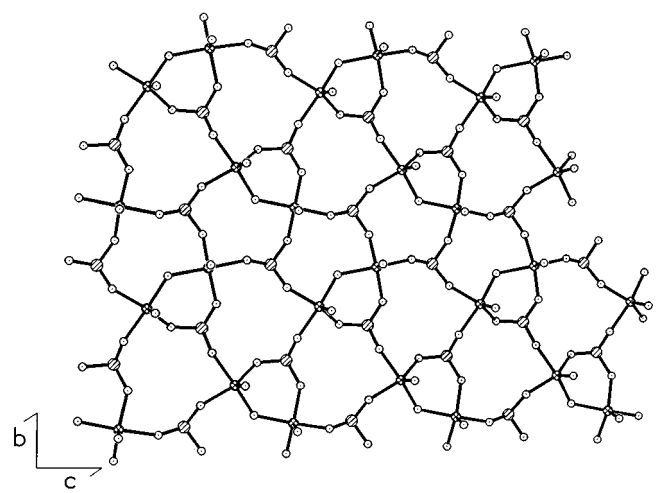

FIG. 2. A view of $Cs[(VO)_2(OH)(O_3PCH_2CH_2PO_3)]$ **1**, along the *a* axis and normal to the V/P/O layer, illustrating the 6-, 10-, and 12-member rings present in the layer. The organic spacers have been omitted for clarity.

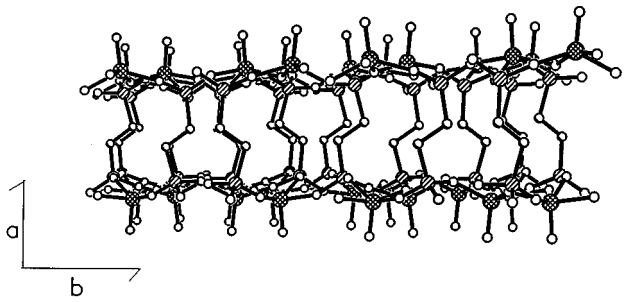

FIG. 3. A view of $Cs[(VO)_2(OH)(O_3PCH_2CH_2PO_3)]$ **1**, normal to the *a* axis illustrating the linkage of the V/P/O layer via the ethylene diphosphonate ligand.

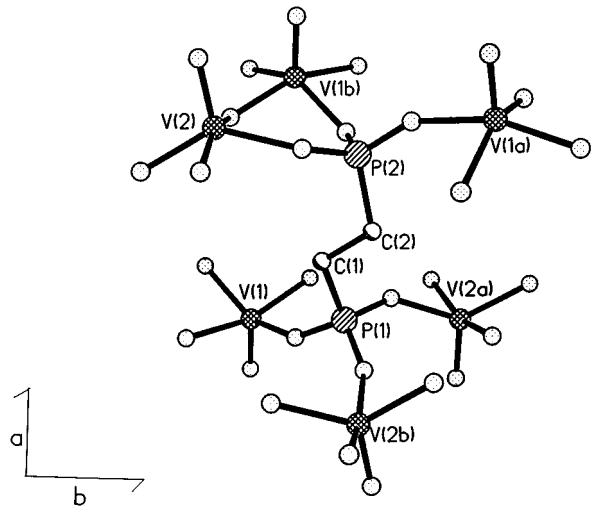

FIG. 4. A view of the coordination of the ethylene diphosphonate ligand in $Cs[(VO)_2(OH)(O_3PCH_2CH_2PO_3)]$ **1**.

observation is in sharp contrast to a layered solid with similar composition. The oxo-vanadium organodiphosphonate $Cs[(VO)_2\ V(O_3PCH_2PO_3)_2(H_2O)_2]$ (12) is synthesized with similar precursors to the title compound **1** but possesses a significantly different structure. The most prominent anomaly is the position of the Cs^+ cations. In $Cs[(VO)_2V(O_3PCH_2PO_3)_2(H_2O)_2]$, the cations are found within the layers with only aquo groups protruding into the interlamellar regions. In contrast, in the title compound **1** the Cs^+ cations were found to occupy sites in the interlamellar region, as noted in Fig. 5. This result may be due to the increased size of the organic spacer in the ethylenediphosphonate ligand in **1**, compared to the methylenediphosphonate ligand in $Cs[(VO)_2V(O_3PCH_2PO_3)_2(H_2O)_2]$. Increasing the size of the organic tether increases the separation between the inorganic V/P/O layers. The stabilizing interactions between the Cs^+ cations and the oxygen atoms of the layer might be decreased due to this increase in separation. Moving into the interlamellar region could allow for enhanced Cs–O interaction and concomitant stabilization of the structure.

The temperature dependent magnetic susceptibility data for $Cs[(VO)_2(OH)(O_3PCH_2CH_2PO_3)]$ exhibit Curie–Weiss paramagnetism at high temperature ($T > 135$ K) with fitted

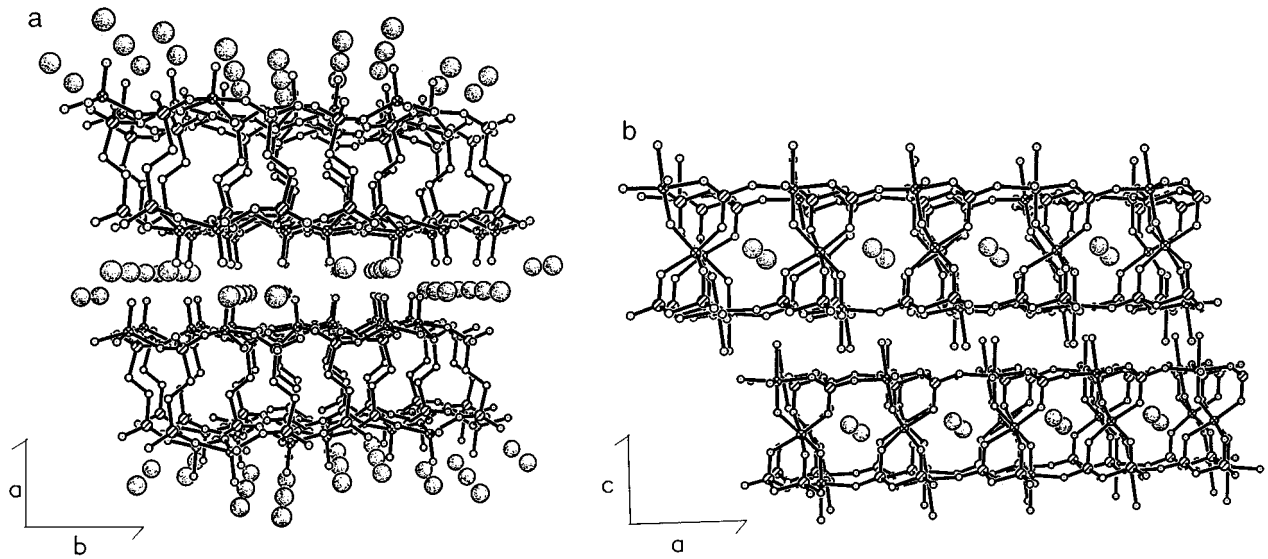

FIG. 5. (a) A view of the structure of $Cs[(VO)_2(OH)(O_3PCH_2CH_2PO_3)]$ **1**, perpendicular to the *a* axis, illustrating the interlamellar occupation of Cs^+ cations. (b) A view of the structure of $Cs[(VO)_2V(O_3PCH_2PO_3)_2(H_2O)_2]$, illustrating the intralamellar occupation of Cs^+ cations.

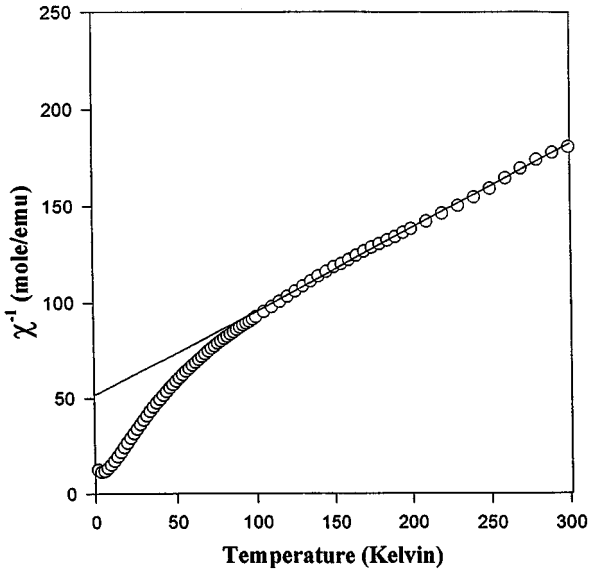

FIG. 6. The inverse magnetic susceptibility of $Cs[(VO)_2(OH)(O_3PCH_2CH_2PO_3)]$ plotted as a function of temperature over the 1.7–300 K temperature region. The line drawn through the data is the fit to the Curie–Wiess model as described in the text.

parameters: $C = 2.30$ emu K/mole, $\theta = -119.21$ K, and $g = 2.14$. The inverse magnetic susceptibility data are plotted in Fig. 6 with the fitted curve. In Fig. 7, at lower temperature, the magnetic susceptibility exhibits a broad maximum consistent with short-range magnetic coupling. The magnetic data were analyzed in the vicinity of the maximum using a model that assumes coupling of two $S = 1/2$ vanadium(IV) centers. The isotropic coupling of these two centers gives the magnetic susceptibility equation

$$\chi = [N_g\mu_\beta^2/kT\,]\,[2e^{2x}/(1 + 3e^{2x})] \qquad [1]$$

where $x = J/kT$.

The magnetic data also required the correction using the molecular field approximation due to secondary interactions, either from interdimer coupling or from zero field splitting of the $S = 1/2$ multiplet. The secondary interactions were treated using the molecular field approximation as

$$\chi = \chi'/[1 - (2zJ'/N_g^2\mu_\beta^2)\chi'], \qquad [2]$$

where χ' is the magnetic susceptibility of the material in the absence of the exchange field (Eq. [1]) and χ is the molecular field influenced magnetic susceptibility that is actually measured. The exchange field coupling parameter is zJ', where z is the number of exchange coupled neighbors. The addition of the molecular field exchange correction resulted in a substantial improvement of the fit to the data. The magnetic susceptibility of $Cs[(VO)_2(OH)(O_3PCH_2CH_2PO_3)]$ was fit to Eq. [1] corrected by Eq. [2] and gave the following parameters: $g = 2.15$, $J/k = -2.5$ K, $zJ'/k = -2.9$, TIP = 0.00234.

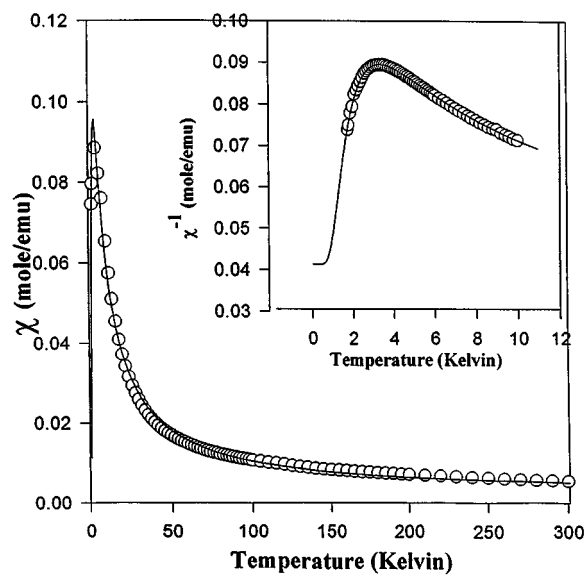

FIG. 7. The magnetic susceptibility of $Cs[(VO)_2(OH)(O_3PCH_2CH_2PO_3)]$ plotted as a function of temperature over the 1.7–300 K temperature region. The curve drawn through the data is the fit to the binuclear model as described in the text. (Inset) Data and fit derived from Eqs. [1] and [2].

CONCLUSION

The title compound has been found to be a layered material with a network of inorganic V/P/O layers which are separated by a layer of organic $\{-CH_2-CH_2-\}$ spacers. Each individual bilayer is separated from the next by a plane of Cs^+ cations. The inorganic layers consist of $\{VO_5\}$ square pyramids and $\{CPO_3\}$ tetrahedra, with the polyhedra arranged so as to form 6-, 10-, and 12-member ring systems. The solid appears to possess discrete hydrophilic and hydrophobic regions. Increasing the length of the organic spacer of the diphosphonate ligand seems to force the cesium cation out of the layer and into the interlamellar region, which may be more accommodating to the cation due to its greater hydrophilicity. Investigations on organodiphosphonates with longer organic spacers is ongoing.

ACKNOWLEDGMENT

This work was funded by a grant from the National Science Foundation, CHE9617232.

REFERENCES

1. J. Zubieta, *Comments Inorg. Chem.* **16,** 153 (1994) and references therein.
2. Q. Chen, J. Salta, and J. Zubieta, *Inorg. Chem.* **32,** 4485 (1993).
3. C. Bhardwaj, H. Hu, and A. Clearfield, *Inorg. Chem.* **32,** 4294 (1993) and referencestherein.
4. K. Segawa, N. Kihara, and H. Yamamoto, *J. Mol. Cat*. **74,** 213 (1992).
5. A. Clearfield, "Inorganic Ion Exchange Materials." CRC Press: Boca Raton, FL, 1982.
6. A. Clearfield and C. Y. Ortiz-Avila, *Supramolecular Architecture*, *ACS Symp. Ser*. **499,** 178 (1992).
7. G. H. Huan, A. J. Jacobson, J. W. Johnson, and J. S. Merola, *J. Solid State Chem.* **89,** 220 (1990)
8. J. W. Johnson, A. J. Jacobson, W. M. Butler, S .E. Rosenthal, J. F. Brody, and J. T. Lewandowski, *J. Am. Chem. Soc*. **111,** 381 (1989).
9. G. H. Huan, A. J. Jacobson, J. W. Johnson, and E. W. Corcoran, *Chem. Mater*. **2,** 91 (1990).
10. M. I. Kahn, Y. Lee, C. J. O'Conner, R. C. Haushalter, and J. Zubieta, *Inorg. Chem.* **33,** 3855 (1994).
11. M. I. Kahn, Y. Lee, C. J. O'Conner, R. C. Haushalter, and J. Zubieta *J. Am. Chem. Soc*. **116,** 4525 (1994).
12. G. H. Bonavia, R. C. Haushalter, C. J. O'Conner, and J. Zubieta, *Inorg. Chem.* **35,** 5603 (1996)
13. N. Walker and D. Stuart, *Acta. Crystallogr. Sect. A* **39,** 158 (1983).
14. *teXsan*: *Texray Structural Analysis Package* (revised). Molecular Structure Corporation, The Woodlands, TX 1992.
15. D. T. Cromer and J. T. Waber, "International Tables for X-Ray Crystallography," Vol. IV. Kynoch Press, Birmingham, England, 1974.
16. D. C. Creagh and J. W. J. McAuley, "International Tables for X-Ray Crystallography," Vol. C, Table 4,2.6.8. Kluwer Academic, Boston, 1992.
17. SHELXTL PC™. Siemens Analytical X-Ray Instruments, Inc., Madison, WI, 1990.
18. C. J. O'Conner, *Prog. Inorg. Chem.* **29,** 203 (1982).
19. J. Gopalakrishnan, *Chem. Mater*. **7,** 1265 (1995)
20. V. Soghomonian, R. C. Haushalter, and J. Zubieta, *Chem. Mater*. **7,** 1648 (1995).
21. V. Soghomonian, R. Diaz, R. C. Haushalter, C. J. O'Conner, and J. Zubieta, *Inorg. Chem.* **34,** 4460 (1995).
22. V. Soghomonian, Q. Chen, R. C. Haushalter, and J. Zubieta, *Angew. Chem. Int. Ed. Engl.* **34,** 223 (1995).
23. I. D. Brown, "Structure and Bonding in Crystals" (M. O'Keefe and A. Navrotsky Eds.), Vol. 11, pp 1–30. Academic Press, New York, 1981.